

Effect of post-homogenization cooling rate and Mn addition on Mg₂Si precipitation and hot workability of AA6060 alloys

Xiaoming Qian¹, Nick Parson², X.-Grant Chen^{1,*}

¹ Department of Applied Sciences, University of Quebec at Chicoutimi,
Saguenay, QC, G7H 2B1, Canada
(*Corresponding author: xgrant_chen@uqac.ca (X.-Grant Chen))

² Arvida Research and Development Centre, Rio Tinto Aluminum,
Saguenay, QC, G7S 4K8, Canada

Abstract

The microstructure evolution for different post-homogenization cooling rates and the flow stress behavior in direct chill cast AA6060 alloys were studied. Results revealed that decreasing cooling rates reduced the flow stress owing to the precipitation of Mg₂Si and reduction of the solid solution level. Micro-alloying of Mn generated a distribution of α -Al(FeMn)Si dispersoids during the homogenization, with the size and number density decreasing at higher homogenization temperatures. TEM studies confirmed that the dispersoids acted as favorable nucleation sites for Mg₂Si and significantly promoted the precipitation of Mg₂Si during subsequent cooling. The high-temperature flow stress was controlled by the solid solution levels of Mg, Si, and Mn resulting from the interaction between dispersoids and Mg₂Si. The combination of the Mn addition, a low cooling rate, and a low homogenization temperature provided the lowest flow stress, which improved the hot workability of the alloy and promoted ready dissolution of Mg₂Si during extrusion.

Keywords

AA6060 alloys, Post-homogenization cooling, Mn addition, Mg₂Si precipitation, High-temperature flow stress

1 Introduction

Al-Mg-Si 6xxx alloys possess an attractive combination of strength, excellent formability, and corrosion resistance in addition to superior anodizing properties [1, 2]. AA6060 aluminum alloys are widely used for parts with complex cross sections in the automobile and architecture industries, and are typically produced using an extrusion process. In the industrial practice, direct chill cast billets are first homogenized, and then extruded. Homogenization consists of heating, soaking, and cooling stages. During heating and soaking, fragmentation of the constituent particles and precipitation of dispersoids can occur; during the cooling stage, Mg_2Si precipitation occurs. The microstructure changes during homogenization can have an important influence on the hot workability and downstream properties.

Extrusion under a T5 condition is frequently used in the aluminum extrusion industry owing to the economic benefit of low cost production. A T5 extrusion condition refers to the in-situ solution treatment and press quenching of extruded profiles in the extrusion press followed by a subsequent artificial aging [3], and therefore, no specific solution treatment after extrusion is required. Extrusion under a T5 condition can also avoid the negative influence of the high-temperature solution treatment on the distortion of the complex shapes of the extruded profiles [4]. Rapid post-homogenization cooling tends to trap the Mg and Si in the solid solution, resulting in an increase in the flow stress, whereas slow cooling can promote the precipitation of Mg_2Si particles, leading to reduced flow stress and the improvement of the hot workability [4-6]. However, if the precipitated Mg_2Si particles are overly coarse during cooling, it can be difficult to achieve full dissolution during the extrusion, resulting in a partial loss of the potential strengthening in the subsequent ageing step. For these considerations, the amount of Mg_2Si particles precipitated during the post-homogenization cooling should be high to reduce the flow stress [7]; however, the particle size must be small for easy dissolution during extrusion [8].

A small addition of Mn is typically made to 6xxx aluminum alloys to modify the microstructure and control the recrystallization and grain structure. During homogenization, Mn-containing dispersoids (α -Al(FeMn)Si) are frequently formed [9], which can influence the deformation process and act as obstacles to grain boundary migration and dislocation movement [10, 11]. Mn also has a significant influence on the strength of aluminum alloys when present in the solid solution. Li *et al.* [12] found that the increase of Mn solutes in the Al matrix increased the microhardness in the Al-Mn-Mg-Si alloy. Liu [13] reported that with the increasing addition of Mn, the flow

stress increases significantly in the AA6082 alloy. It has also been reported that the dispersoids formed during homogenization can act as heterogeneous nucleation sites for the precipitation of the Mg₂Si phases [14, 15].

Several studies have been performed on the different effects of cooling during homogenization in 6xxx alloys. It was reported that during the cooling stage in an AA6063 alloy, Mg₂Si precipitation was promoted by decreasing the cooling rate from 2000 to 100 °C/h [16]. However, a further decrease in the cooling rate below 100 °C/h led to coarser Mg₂Si particles. It was confirmed that the equilibrium β-Mg₂Si was the predominant phase precipitated during 1000–250 °C/h cooling after homogenization in an AA6082 alloy [17]. Birol [18] reported that a low quenching temperature during cooling led to more Mg₂Si precipitation and resulted in a decrease of the room temperature hardness in 6082 alloy. In our previous work [19], the influence of the homogenization treatment (temperature and soaking time) on the hot workability of AA6060 alloys was investigated. It was found that the flow stress behavior of the homogenized AA6060 alloys was mainly determined by the solid solution level. However, limited studies have focused on the effect of the cooling practice of homogenization on the hot deformation behavior. Moreover, the interaction of heterogeneous nucleation between the dispersoids and Mg₂Si during homogenization remains less understood.

In the present study, the microstructure changes in AA6060 alloys with microalloying of Mn were examined during homogenization as a function of soak temperature and cooling rate with particular emphasis on the role of the dispersoid and Mg₂Si particles. The effects of microstructure on high-temperature flow stress behavior during hot deformation were investigated by hot compression testing.

2 Experimental

Experiments were conducted on two AA6060 alloys, with and without a 0.1 wt% Mn addition. All samples were from direct chill (DC) cast billets with a diameter of 101 mm, provided by the Arvida Research and Development Center, Rio Tinto Aluminum in Saguenay, Quebec. The chemical compositions of the two experimental alloys are listed in Table 1. All samples for microstructural analysis and hot deformation were selected 15 mm away from the cast surface of the billets to avoid possible microstructural and compositional variations. The samples were homogenized at 515, 545, and 575 °C for six hours and cooled at three cooling rates, e.g., water quench, 500 °C/h, and 100 °C/h. The samples were mounted and polished for microstructure observation. To reveal the

microstructure details, the polished samples were etched with a 0.5% HF solution for 40 s. The microstructure examination was performed using optical microscopy, scanning electron microscopy (SEM, JEOL-6480LV), and transmission electron microscopy (TEM, JEM-2100). Quantitative image analysis for the Mg₂Si and dispersoid distributions was performed based on SEM images of etched samples. The electrical conductivity (EC) of the samples was measured at room temperature after immediately completing the homogenization using a Sigmascope SMP10 eddy current device. The average value of each sample was determined from five measurements.

For the hot deformation testing, cylindrical specimens of 10 mm diameter and 15 mm height were machined from the DC cast billets after homogenization. Uniaxial hot compression tests were performed at 400 and 500 °C with strain rates of 1 s⁻¹ using a Gleeble 3800 thermo-mechanical testing unit. The specimens were heated at a rate of 2 °C/s to the desired temperature and held for 180 s to ensure a uniform temperature distribution. The specimens were deformed to a total true strain of 0.75 followed by a water quench.

Table 1 Chemical compositions of two experimental alloys (wt.%)

| Alloys | Mg | Si | Fe | Mn | Al |
|-------------|------|------|------|------|------|
| Base alloy | 0.37 | 0.50 | 0.17 | - | Bal. |
| 0.1Mn alloy | 0.37 | 0.51 | 0.19 | 0.10 | Bal. |

3 Results

3.1 Microstructures

3.1.1 As-cast microstructures

The as-cast microstructures for the base and 0.1Mn alloys are displayed in Fig. 1. As indicated, the as-cast microstructure of the base alloy (Fig. 1a) was composed of aluminum dendrite cells (Al matrix), large plate-like β-AlFeSi intermetallic (gray), and primary Mg₂Si particles (dark) distributed along the dendrite boundaries. For the 0.1Mn alloy (Fig. 1b), the microstructure was similar to the base alloy indicating that the presence of 0.1% Mn had almost no influence on the as-cast microstructure.

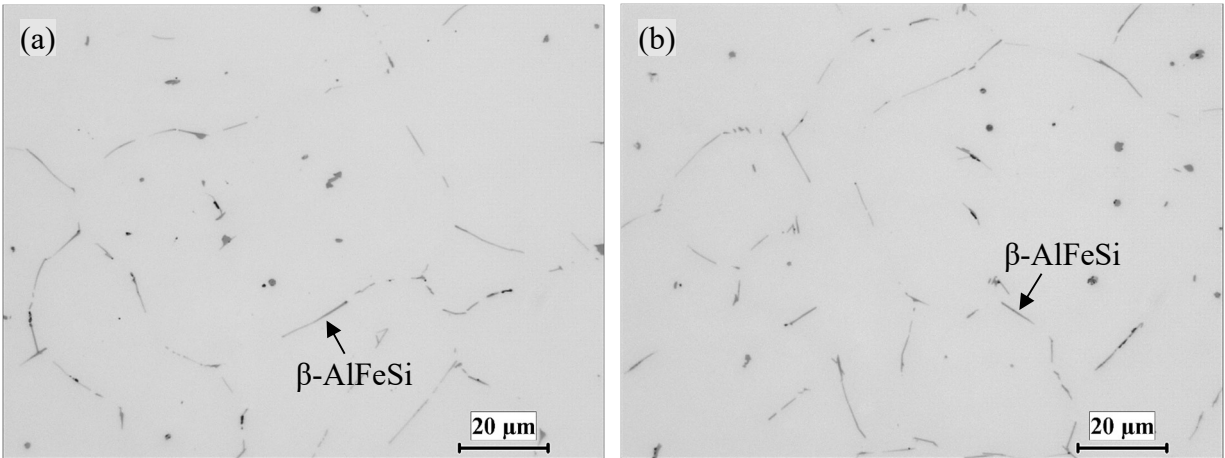


Fig. 1 As-cast microstructures of (a) the base alloy and (b) 0.1Mn alloy

3.1.2 Microstructures after homogenization with water quench

The homogenized microstructures of the base and 0.1Mn alloys with the fastest cooling rate (water quench) are displayed in Fig. 2. In general, fragmentation of the intermetallics was observed in both alloys. Large plate-like β -AlFeSi particles were replaced by more rounded and separate particles, which were α -AlFeSi in the base alloy (Fig. 2a) and α -Al(FeMn)Si in the 0.1Mn alloy (Fig. 2b, c, and d). In the base alloy, there was no phase precipitation in the aluminum matrix (Fig. 2a). Conversely, a number of dispersoids were formed in the 0.1Mn alloy (Fig. 2b, c, and d). The number density of the dispersoids decreased with increasing homogenization temperature. Furthermore, a nonuniform distribution of dispersoids was observed with preferential precipitation near the interdendritic region. The dispersoids were closely observed by SEM; the images are inserted in Fig. 2b and c.

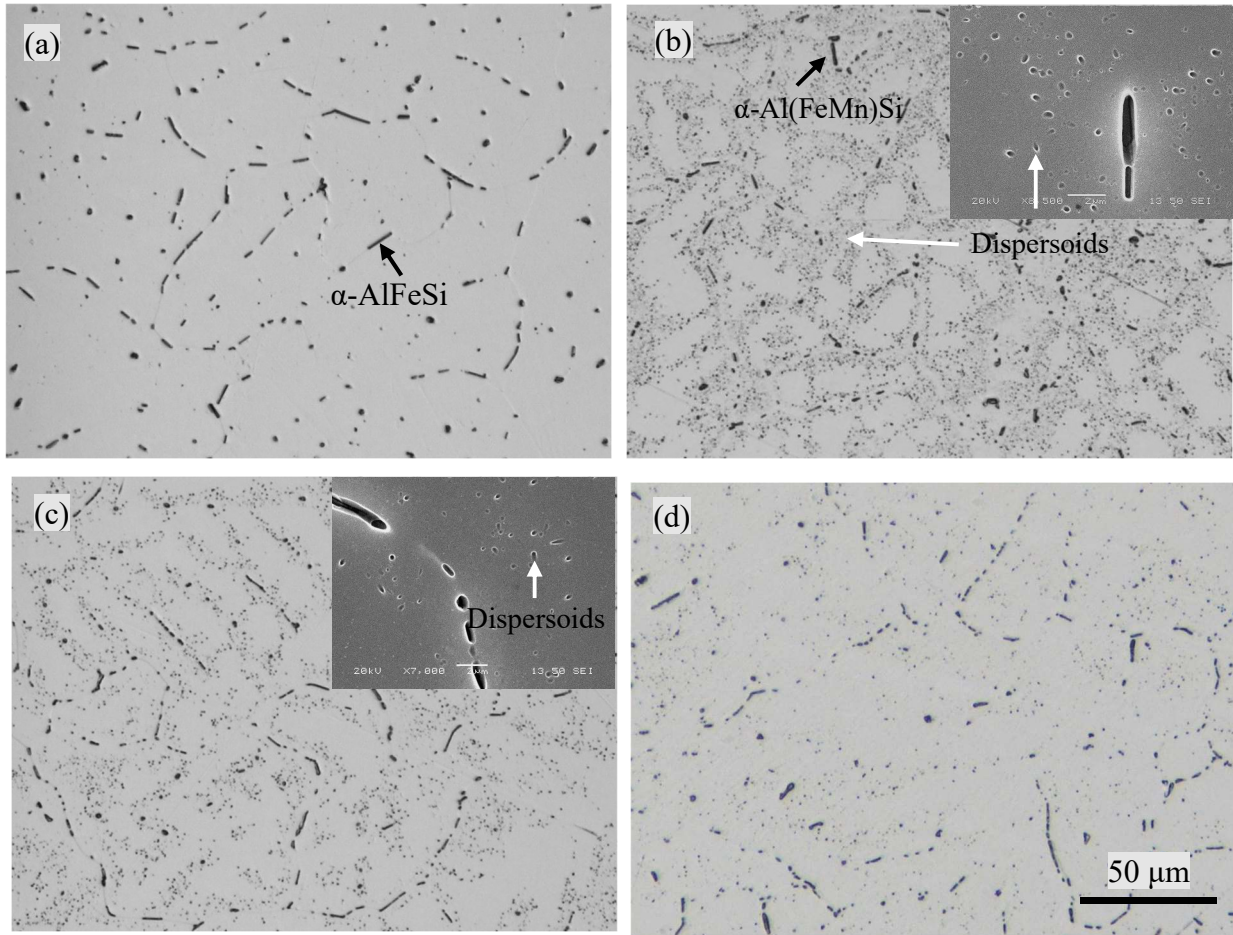


Fig. 2 Microstructures of homogenized samples with water quench: (a) base alloy homogenized at 545 °C, (b–d) 0.1Mn alloy homogenized, (b) at 515 °C, (c) at 545 °C, and (d) at 575 °C. SEM images displaying dispersoids are inserted in b and c.

Fig. 3a shows a bright field TEM image of typical dispersoids in the 0.1Mn alloy after homogenization at 545 °C for 6 h with a water quench. The dispersoids are present in short plate and rod forms, which can be attributed to the projection of the plate-like morphology in a 2D image. Based on the TEM–EDX analysis (Fig. 3b), the dispersoids were identified as α -Al(FeMn)Si, which corresponds with earlier works [10, 13]. Fig. 4 displays the evolution of the number density and equivalent diameter of the dispersoid particles measured by image analysis on a series of SEM images. With increasing homogenization temperature from 515 to 575 °C, both the number density and size of the dispersoids decreased, consistent with a dissolution process.

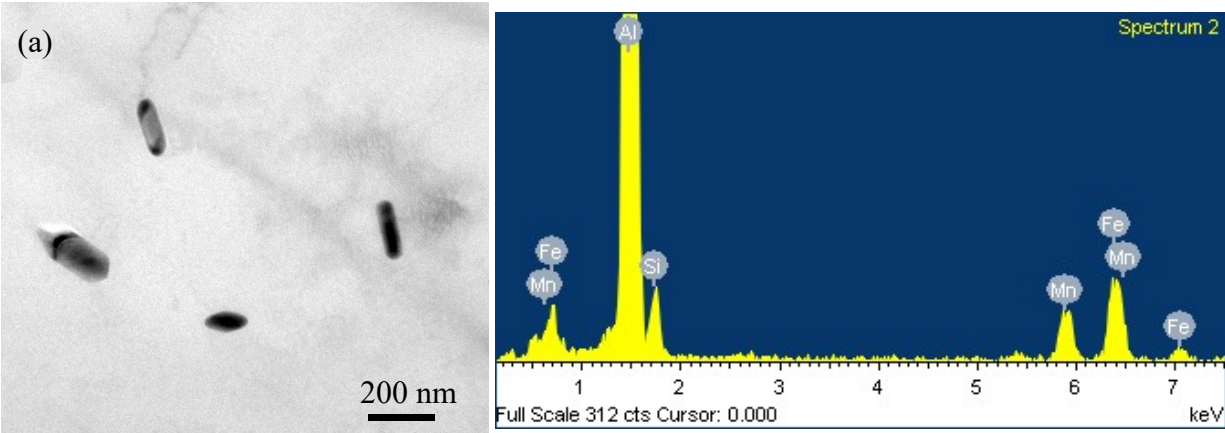


Fig. 3 (a) TEM bright field image showing the dispersoids and (b) TEM-EDX results of dispersoids in 0.1Mn alloy after homogenization at 545 °C for 6 h.

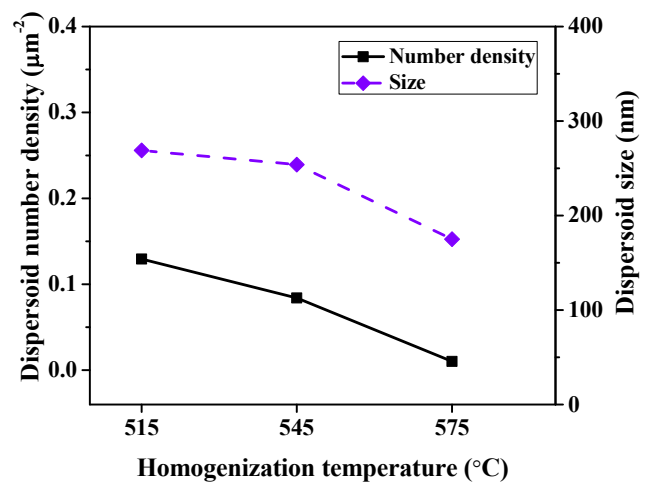


Fig. 4 Number density and size of dispersoids in the 0.1Mn alloy at different homogenization temperatures

3.1.3 Microstructures after homogenization with 500 °C/h and 100 °C/h cooling rates

The microstructures of the base and 1Mn alloys after homogenization at 545 °C and cooling at 100 °C/h are displayed in Fig. 5. The precipitation of Mg₂Si was observed in the aluminum matrix of both alloys. For the base alloy (Fig. 5a), when compared to the water-quenched samples (Fig. 2a), it is evident that a high number of Mg₂Si particles

precipitated inside the matrix. In the 0.1Mn alloy (Fig. 5b), the precipitation of the Mg_2Si was mixed with the pre-existing dispersoids. Compared to the base alloy, an overall greater number density and finer size of the Mg_2Si particles were observed.

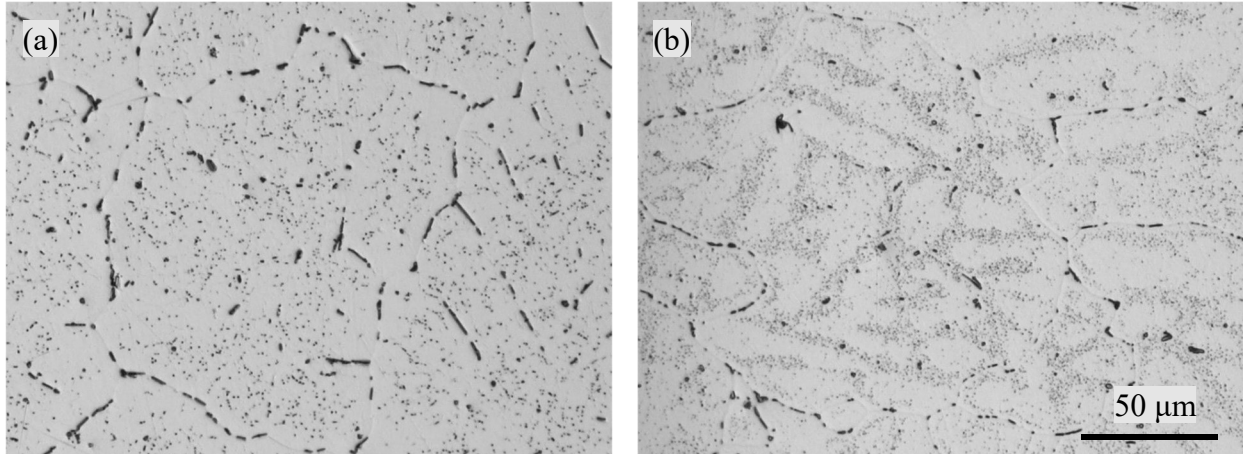


Fig. 5 Microstructures of (a) base alloy and (b) 0.1Mn alloy homogenized at 545 °C for 6 h with 100 °C/h cooling.

Fig. 6 displays a series of typical SEM images indicating the precipitation of the Mg_2Si in the base and 0.1Mn alloy after different homogenization conditions. In general, the Mg_2Si particles exhibited a rod-like morphology and a clear change in size and number density as a function of the Mn content and homogenization conditions. A greater number density and finer Mg_2Si particle size were observed in the 0.1Mn alloy compared to the base alloy. Quantitative analysis of the Mg_2Si particles was performed based on the SEM images. The Mg_2Si number density was calculated as the number of Mg_2Si particles in a unit area including the region having less particle distribution. The size of the Mg_2Si was defined as the length of the rod-like Mg_2Si particles. Fig. 7 displays the evolution of the number density and size of the Mg_2Si particles. In general, for both alloys, the low cooling of 100 °C/h resulted in a greater number density and larger size of Mg_2Si than a faster cooling of 500 °C/h. Moreover, the 0.1Mn alloy produced a greater Mg_2Si number density and smaller size than the base alloy under the same homogenization condition. In the base alloy (Fig. 7a), the Mg_2Si number density and size remained virtually unchanged with the increasing homogenization temperature. However, in the 0.1Mn alloy (Fig. 7b), the Mg_2Si number density decreased and the size increased marginally with increasing homogenization temperatures.

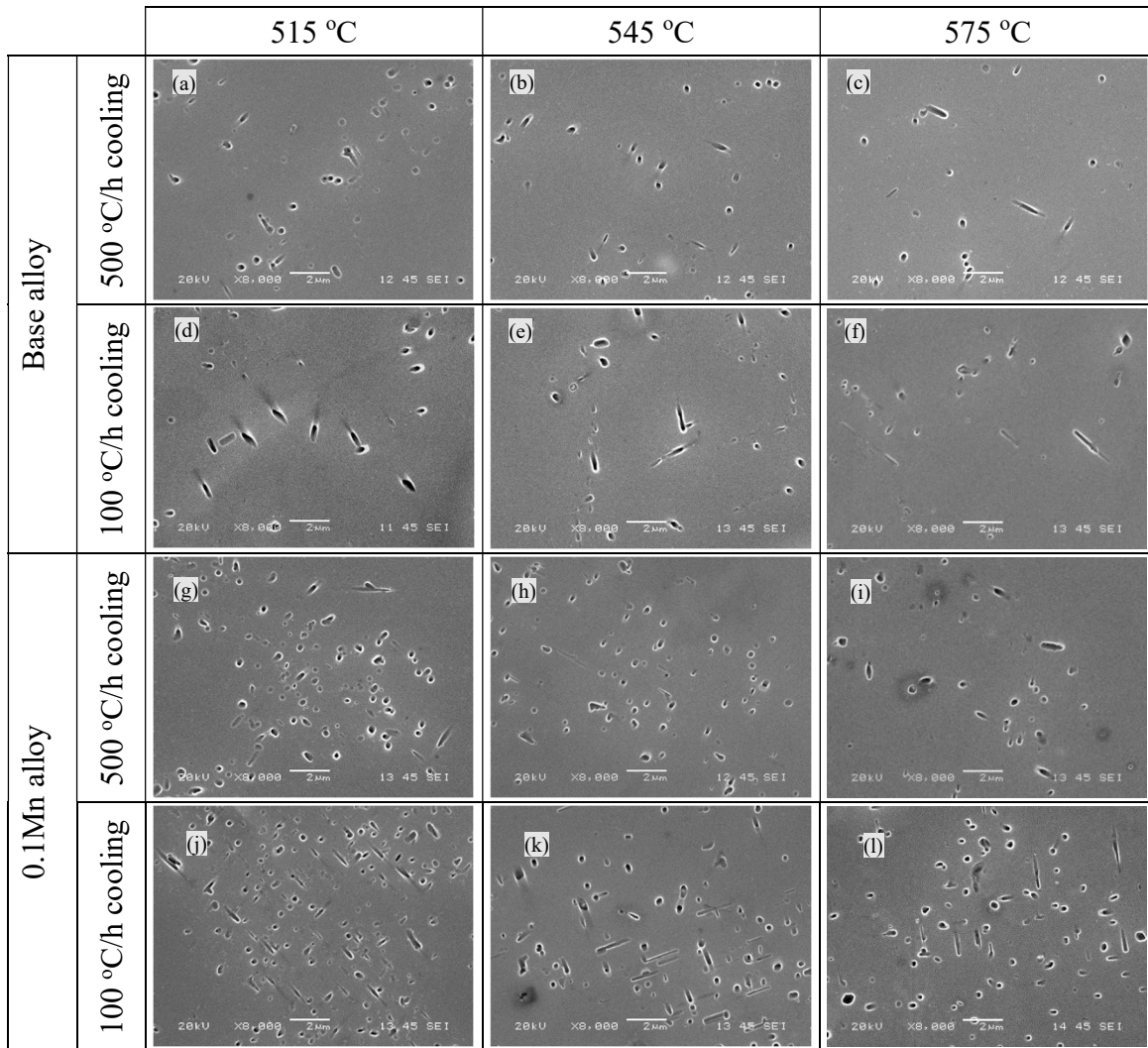


Fig. 6 Mg₂Si precipitation in base and 0.1Mn alloy for different homogenization conditions

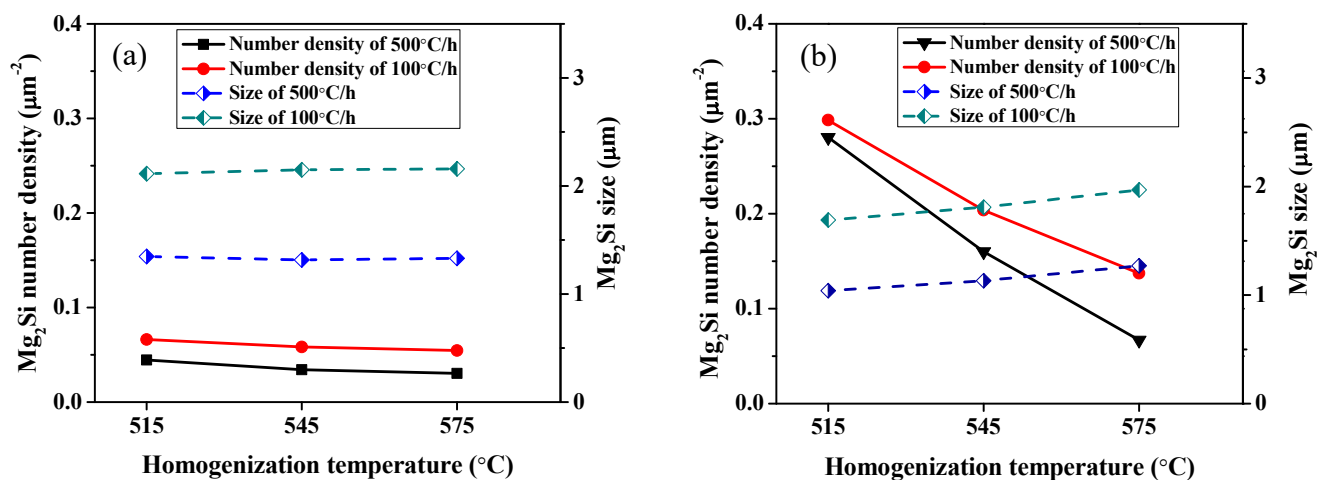


Fig. 7 Number density and size of Mg₂Si particles in (a) base alloy and (b) 0.1Mn alloy with different cooling rates and homogenization temperatures.

3.2 Electrical conductivity and solid solution level

The electrical conductivity after homogenization was used to monitor the solid solution level in the aluminum matrix. Fig. 8 illustrates the influence of the cooling rate and homogenization temperature on the electrical conductivity. In both alloys, the electrical conductivity increased with decreasing cooling rates owing to the precipitation of the Mg₂Si, and hence, the reduced solid solution level. However, the changes in electrical conductivity with cooling rate for the 0.1Mn alloy were greater than those in the base alloy. For example, at a fixed homogenization temperature of 545 °C, the electrical conductivity decreased by 2.55% IACS in the base alloy as the cooling rate shifted from the water quench to the 100 °C/h cooling rate, whereas the change in electrical conductivity of the 0.1Mn alloy was 3.67% IACS, which is 30.5% greater than that of the base alloy. The greater change in the electrical conductivity in the 0.1Mn alloy reflects a greater amount of Mg₂Si precipitation at the same cooling condition owing to the nucleation on the α -Al(FeMn)Si dispersoids (Fig. 6). In the base alloy, the electrical conductivity remained virtually unchanged with increasing homogenization temperature, indicating the limited influence of homogenization temperature on the solid solution level, which is associated with a constant number density and size of the Mg₂Si (Fig. 7a). However, the electrical conductivity in the 0.1Mn alloy decreased with the increasing homogenization temperature. This was believed to be related to the dissolution of the dispersoids at high temperatures and the increased level of Mn solid solution (Fig. 2b, c, d, and Fig. 4).

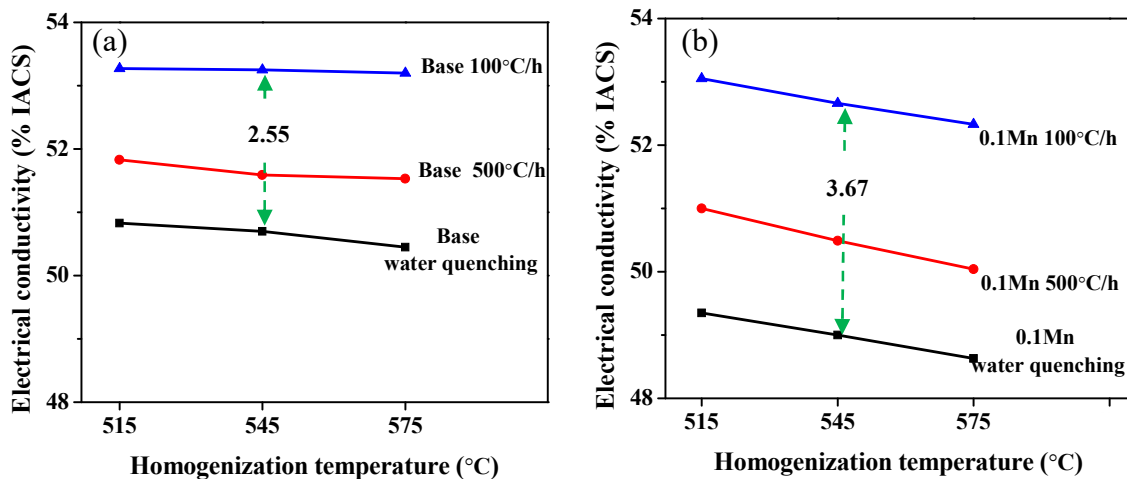


Fig. 8 Electrical conductivity as a function of the cooling rate and homogenization temperature: (a) base alloy and (b) 0.1Mn alloy.

3.3 High temperature flow stress

To study the hot workability of the experimental alloys, compression tests were performed at temperatures of 400 °C and 500 °C with a strain rate of 1 s⁻¹. The samples homogenized at 575 °C were chosen to illustrate typical true stress-true strain curves; these are displayed in Fig. 9.

In the majority of cases, the flow stress increased sharply at the start of deformation owing to the dislocation multiplication and the high rate of work hardening [20, 21]. Shortly afterwards, the flow stress experienced a slow increase until the end of the deformation process, indicating the balance between the dynamic work hardening and dynamic softening. It was evident that the flow stress was temperature dependent, and the deformation at 400 °C indicated higher flow stress levels than at 500 °C. The elevated flow stress at lower deformation temperature was due to a stronger dynamic work hardening, which is a general trend in hot deformation [22].

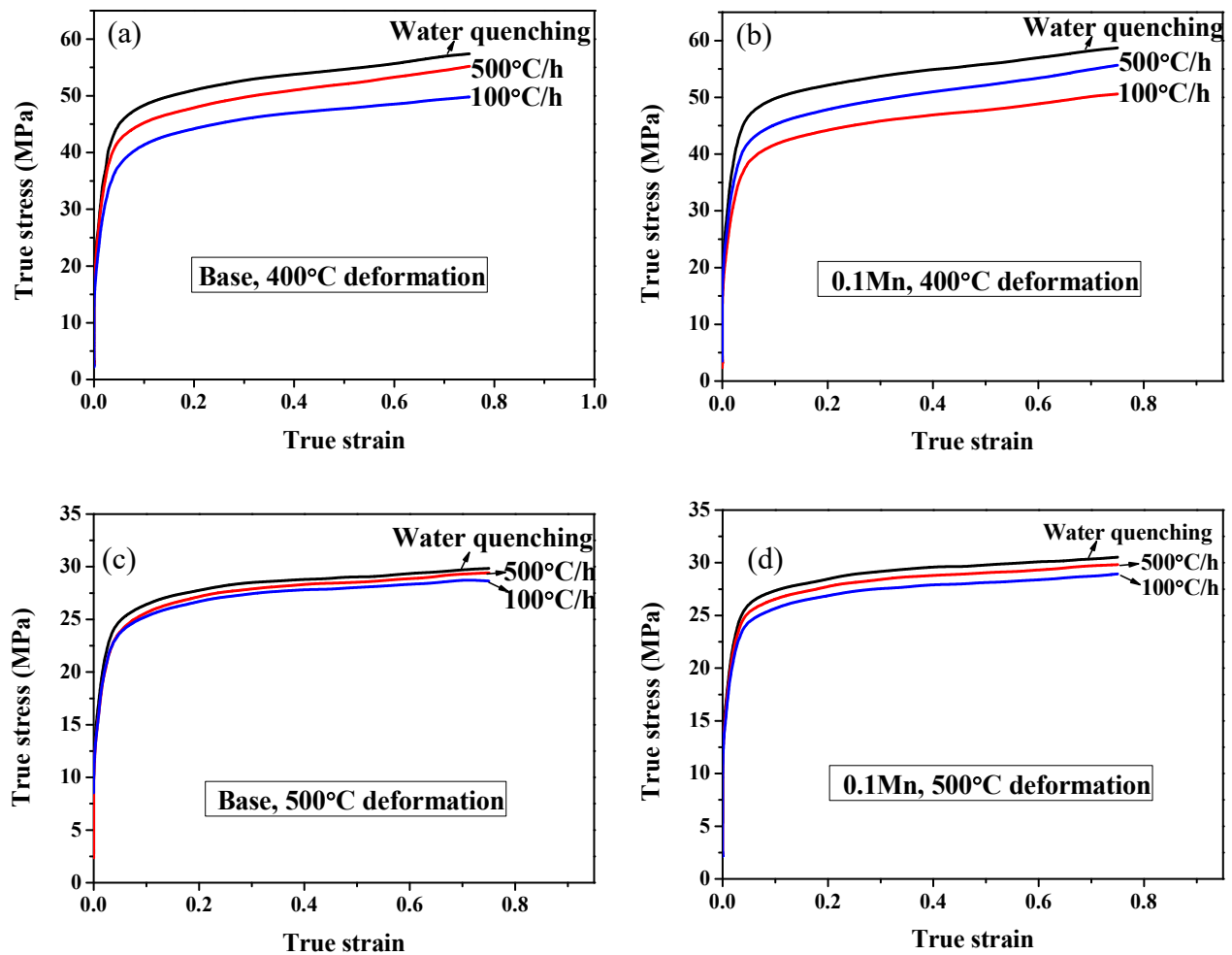


Fig. 9 True stress-true strain curves of samples after 575 °C homogenization with 1 s⁻¹ strain rate: the base alloy (a) deformed at 400 °C and (c) deformed at 500 °C; the 0.1Mn alloy (b) deformed at 400 °C and (d) deformed at 500 °C.

To better compare the effect of the cooling rate and homogenization temperature on the hot workability, the flow stress values at a strain of 0.75 are plotted in Fig. 10. It is evident that the flow stress decreased with reduced cooling rate at deformation temperatures of 400 and 500 °C. The trends with the homogenization temperature and cooling rate were similar for the two deformation temperatures. This suggests that although the high deformation temperature of 500 °C was greater than the Mg₂Si solvus of approximately 470 °C, the rapid heat to the test temperature and short soak time before deformation was insufficient to dissolve the Mg₂Si particles produced by the homogenization. The water-quenched samples provided the highest flow stress, whereas the samples with the lowest cooling rate of 100 °C/h exhibited the lowest flow stress for both alloys. Moreover, the flow stress of the base alloy indicated low sensitivity to the homogenization temperature (Fig. 10a and c), whereas in the case of the 0.1Mn alloy (Fig. 10b and d), the flow stress increased moderately with increasing homogenization temperature. Changes in cooling rate resulted in different flow stress responses for the two alloys. For example, with the homogenization temperature of 545 °C and deformation at 400 °C, the increment in flow stress between the water quench and 100 °C/h cooling was 6.9 MPa for the base alloy (Fig. 10a), whereas for the 0.1Mn alloy, a greater decrease of 8.4 MPa was observed (Fig. 10b). The wider variation for the Mn containing alloy was likely due to the enhanced Mg₂Si precipitation on the dispersoids at low cooling rates and the increased Mn in solid solution for the water-quenched condition. It is clear that overall the flow stress behavior demonstrated a similar yet reversed tendency with the electrical conductivity when compared the results between Fig. 10 and Fig. 8, suggesting that the high-temperature flow stress was closely related to the solid solution levels [19].

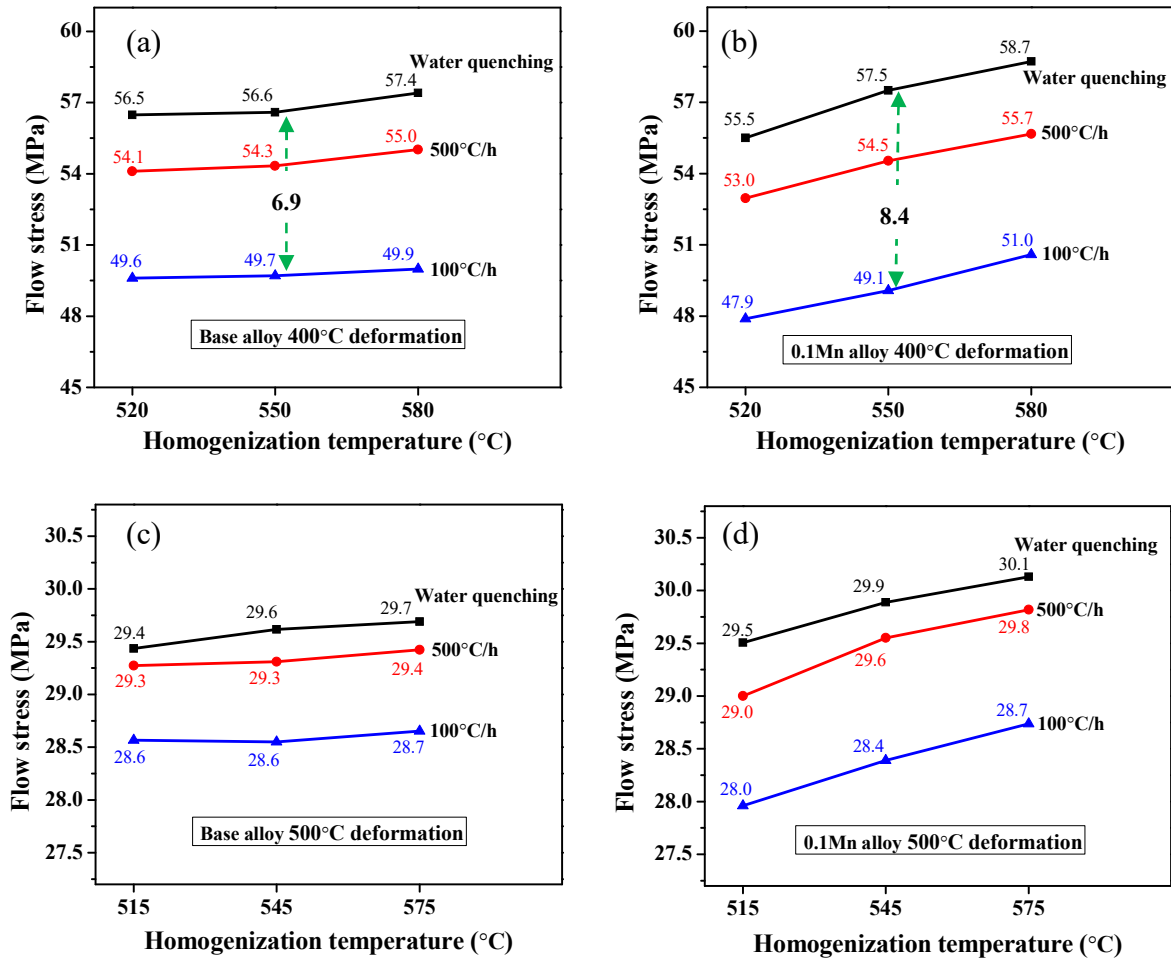


Fig. 10 Flow stresses at 0.75 strain as a function of cooling rate and homogenization temperature: the base alloy (a) deformed at 400 °C and (c) deformed at 500 °C; the 0.1Mn alloy (b) deformed at 400 °C and (d) deformed at 500 °C.

4 Discussion

Two AA6060 aluminum alloys (base and 0.1Mn) were studied and the results revealed that the water quench samples retained virtually all of the Mg and Si in solution, whereas the samples with post-homogenization cooling rates of 500 and 100 °C/h contained Mg₂Si precipitates formed during the cooling. It has been reported that solute elements can significantly influence the hot deformation behavior of aluminum alloys by hindering the dislocation movement and the creation of pile-ups [23, 24], which in turn leads to a significant hardening and contributes to an increase in flow stress [25, 26].

4.1 Effect of cooling rate and dispersoids on Mg₂Si precipitation and flow stress

In the present study, the cooling rate had a predominant role controlling the Mg and Si solid solution levels in the aluminum matrix and hence, the flow stress. For both alloys, the water quench after homogenization suppressed any Mg₂Si precipitation and resulted in the highest level of Mg and Si in solution and hence, the highest flow stress. Cooling at the intermediate rate of 500 °C/h promoted Mg₂Si precipitation (Fig. 7), the solid solution level in the matrix decreased and the flow stress decreased correspondingly (Fig. 10). Decreasing the cooling rate to 100 °C/h resulted in increased Mg₂Si precipitation and a further decrease in the flow stress (Fig. 10) owing to the even lower solid solution level in the matrix (Fig. 7).

In the 0.1Mn alloy, α -Al(MnFe)Si dispersoids precipitated during homogenization (Fig. 2b, c, and d) and acted as nucleation sites for Mg₂Si formation during the cooling. For the same cooling conditions (500 °C/h or 100 °C/h), the 0.1Mn alloy always produced a greater Mg₂Si particle number density and finer size compared to the base alloy free of dispersoids. The enhanced Mg₂Si precipitation, in turn, reduced the Mg and Si solid solution levels and further decreased the flow stress (Fig. 10). However, with increasing homogenization temperature, the dispersoid number density decreased owing to dissolution (Fig. 4), resulting in a corresponding decrease in the Mg₂Si number density and an increase in particle size (Fig. 7b). This contributed to a flow stress increase with homogenization temperature for the Mn containing alloy (Fig. 10b and d).

A comparison of the flow stress values for the Mn free and Mn containing alloys for both deformation temperatures in Fig. 10 reveals a difference in behavior based on the homogenization temperature. At the lowest homogenization temperature (515 °C), the Mn containing alloy provide a reduced flow stress for all cooling rates, whereas for homogenization at the highest temperature of 575 °C, the Mn containing alloy always provided the highest flow stress. This can be rationalized in terms of the Mn dispersoid formation. At 515 °C, a high density of dispersoids was produced providing a low level of Mn in solid solution. Furthermore, the dispersoids promoted Mg₂Si precipitation, providing the low level of Mg and Si in solution and resulting in a reduced flow stress. Conversely, at 575 °C, the Mn solid solution level was higher resulting in a lower density of dispersoids for cooling rates of 500 and 100 °C/h, the Mg₂Si particle density was only marginally greater than for the base alloy. In this situation, the Mg and Si levels in solution were similar, with the Mn solid solution level dominating the flow stress behavior. This is reflected in the fact that after the water quench, where all the Mg and Si were held in solution, the flow stress of the Mn containing alloy was greater than the

base alloy. These results clearly indicate that the presence of the dispersoids resulting from the Mn microalloying in AA6060 alloy promoted Mg_2Si precipitation during the cooling, and reduced the high-temperature flow stress, which is beneficial for extrudability.

TEM investigation revealed a close nucleation and growth relationship between the dispersoids and Mg_2Si during post-homogenization cooling (Fig. 11). In the 0.1Mn alloy, as indicated with the arrows, the Mg_2Si particles always precipitated on the pre-existing dispersoids. This phenomenon was observed at both cooling rates (Fig. 11a and b for 100 °C/h and Fig. 11c and d for 500 °C/h). During cooling, the driving force for the Mg_2Si precipitation is the supersaturation of the Mg and Si in the aluminum solid solution. Although the nature of the crystallographic relation between the dispersoids and the Mg_2Si remains less understood, the TEM finding provided strong evidence that the pre-existing dispersoids could act as favorable nucleation sites for the subsequent precipitation of Mg_2Si . The greater the dispersoid density, for example from low temperature homogenization, the greater the number of Mg_2Si particles precipitated and the more uniform the distribution.

The multiple benefits of the nucleation effects between the dispersoids and Mg_2Si are reported in literature; however, the mechanisms are not completely understood. The earlier literature [14] indicates that when Mg_2Si particles first form in the aluminum matrix during the heating stage of the homogenization, the dispersoids can nucleate on the metastable Mg_2Si phase or its transition phase in the Al-Si-Mg 6xxx alloys. It was also reported that Mg_2Si provided an essential condition for the formation of α -Al(MnFe)Si dispersoids in the Al-Mg-Si alloys during heat treatment [27]. Recently, Li *et al.* [28] reported that α -Al(MnFe)Si dispersoids preferentially nucleated and grew in the original orientation of pre-existing β' - Mg_2Si during the heating of 3xxx alloys. Reiso [15] found that Mg_2Si precipitated preferentially on the pre-existing AlFeSi dispersoids in an Al-Mg-Si alloy after extrusion, and the amount of Mg_2Si increased with an increasing number density of the AlFeSi dispersoids.

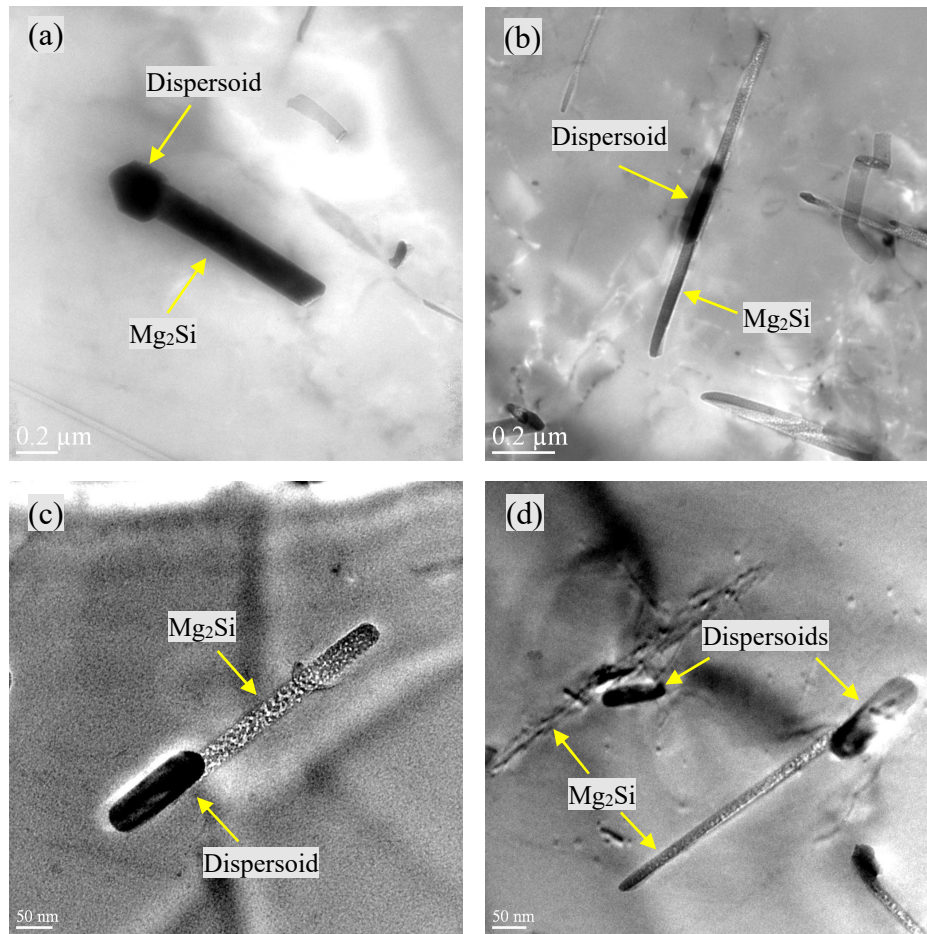


Fig. 11 TEM bright field images indicating that Mg₂Si precipitated and grew on pre-existing dispersoids in 0.1Mn alloy under 515 °C homogenization condition with 100 °C/h cooling rate (a and b) and 500 °C/h cooling rate (c and d).

4.2 Industrial aspect

In the direct hot extrusion process for aluminum alloys, DC cast and homogenized billets are preheated to a selected temperature and then loaded into the press and extruded to obtain the desired profile. Fig. 12 displays the schematic extrusion pressure and temperature curves as the billet passes through the extrusion process [15]. The press force at extrusion breakthrough often is a limiting factor in terms of productivity. The breakthrough force results from a combination of the billet container friction and force required to push the billet through the die. Consequently, the press force is highest at the start of the extrusion when the billet length is the greatest. The lower the breakthrough pressure the greater the extrusion speed that a given press can achieve; this also allows

lower billet temperatures to be used with further gains in productivity. The work performed during extrusion is mainly converted to heat, which results in a temperature increase as the metal passes through the die as indicated in Fig. 12. This is typically controlled such that the product reaches a temperature greater than the Mg_2Si solvus. With the rapid diffusion rates encountered during hot deformation, the Mg_2Si particles in the billet can be dissolved; the extrusion process is used as an in-situ solution treatment for the majority of 6xxx extrusion alloys.

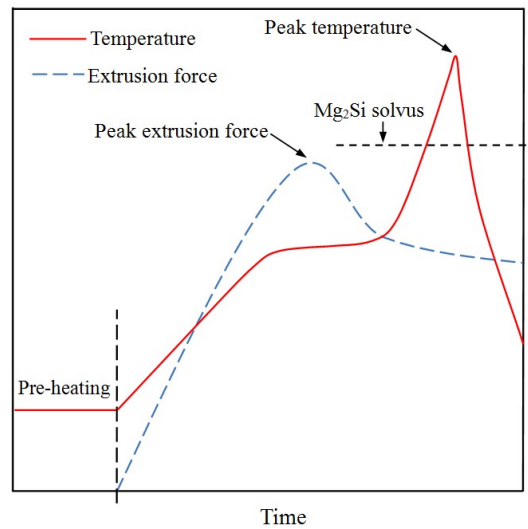


Fig. 12 Schematic of extrusion force and temperature curves during extrusion.

The material flow stress clearly has a direct effect on the extrusion force, the force at breakthrough, and corresponding extrusion productivity. Small differences of few percent can translate into significant improvements in extrusion speed. The present work has demonstrated that the flow stress can be significantly reduced by a lower post-homogenization cooling rate to enhance the Mg_2Si precipitation and reduce Mg and Si solid solution levels. This can be further enhanced with an addition of Mn combined with the correct choice of homogenization temperature.

Regarding Mg_2Si dissolution, a full dissolution of Mg_2Si particles during extrusion is desirable, particularly for the T5 condition, to ensure the sufficient strengthening effect during subsequent aging. In this case, Mg_2Si particles with a high number density and fine size tend to be easily dissolvable at the peak extrusion temperature. If the Mg_2Si particles were overly coarse, their full dissolution would be difficult in the short time of extrusion, resulting in a partial loss of potential strengthening during ageing. The current

study confirmed that the microalloying of 0.1 wt% Mn can reduce the Mg₂Si particle size compared to a Mn free alloy (Fig. 7). In combination with 100 °C/h cooling and homogenization at 515 °C, the 0.1Mn addition produced a greater Mg₂Si particle number density and reduced size (Fig. 7b) than the base alloy resulting in a significantly lower flow stress (Fig. 10). Using a homogenization temperature of 545 °C and commercially achievable cooling rates of 100–500 °C/h, the flow stress for the 0.1Mn alloy was similar to that of the base alloy; however, the Mg₂Si particle number density was greater and the particle was size finer than for the base alloy. This is still advantageous for Mg₂Si dissolution during extrusion. At the highest homogenization temperature (575 °C), the Mg₂Si number density in the 0.1Mn alloy decreased and the particle size increased owing to the coarsening and dissolution of the dispersoids. Although the Mg₂Si particles were finer than in the base alloy, which is beneficial for Mg₂Si dissolution during extrusion, the flow stress was higher than the base alloy owing to the increased Mn in the solid solution, which would be detrimental to extrudability.

5 Conclusions

- 1) During the post-homogenization cooling of AA6060 alloys at commercially relevant rates, Mg₂Si particles precipitated in the aluminum matrix and their number density and size had a significant effect on the solid solution level and high-temperature flow stress.
- 2) At reduced post-homogenization cooling rates, the flow stress decreased owing to the precipitation of Mg₂Si and reduction of solid solution levels. The lowest cooling rate tested (100 °C/h) produced the lowest flow stress corresponding to the maximum precipitation of Mg₂Si.
- 3) Micro-alloying of 0.1 wt% Mn in AA6060 alloys generated a reasonable number of α -Al(FeMn)Si dispersoids during homogenization. These acted as favorable nucleation sites for the Mg₂Si and promoted the precipitation of Mg₂Si during the post-homogenization cooling, resulting in a greater number density and reduced size of the Mg₂Si compared to the base alloy free of Mn.
- 4) The benefits of the micro-alloying of 0.1 wt% Mn varied with the homogenization temperature applied, reflecting the relative effects on the Mg, Si, and Mn solid solution levels:
 - a) At 515 °C, the flow stress was reduced compared to the base alloy and the Mg₂Si particle size was reduced.
 - b) At 545 °C, the flow stress was similar to the base alloy; however, the Mg₂Si

particles size remained reduced.

- c) At 575 °C, the flow stress was increased owing to the Mn solid solution level; however, the Mg₂Si particle size remained finer than the base alloy.

Acknowledgement

The authors would like to acknowledge the financial support from the Natural Sciences and Engineering Research Council of Canada (NSERC) under the Grant CRDPJ 514651-17 through the Research Chair in Metallurgy of Aluminum Transformation at the University of Quebec at Chicoutimi.

References

- [1] J.R. Davis, Aluminum and Aluminum Alloys, ASM International, Materials Park, OH (1993) 59-87.
- [2] J.G. Kaufman, Introduction to Aluminum Alloys and Tempers, ASM International, Materials Park, OH (2000) 87-118.
- [3] L. Aydi, M. Khlif, C. Bradai, S. Spigarelli, M. Cabibbo, M. El Mehtedi, Mechanical properties and microstructure of primary and secondary AA6063 aluminum alloy after extrusion and T5 heat treatment, *Materials Today, Proceedings* 2 (2015) 4890 – 4897
- [4] E.B. Bjornbakk, The influence of homogenization cooling rate, billet preheating temperature and die geometry on the T5-properties for three 6xxx alloys extruded under industrial conditions, *Materials Science Forum* 396-402 (2002) 405-410
- [5] N. Dahl, T. Johnsen, B.R. Henriksen, E.K. Jensen. Precipitation of Mg₂Si in Al–Mg–Si-alloys during cooling from homogenization temperature, *Proceedings of 6th International Aluminum Extrusion Technology Seminar* 1 (1996) 529-535.
- [6] J. Langerweger, Effect of metallurgical factors on productivity in the extrusion of aluminum–magnesium–silicon (AlMgSi) alloys, *Aluminum* 58(1982) 107-109.
- [7] J. van de Langkruis, The effect of thermal treatments on the extrusion behaviour of AlMgSi alloys, PhD Thesis, Delft University of Technology (2000) 61-84.
- [8] Y. Birol, The effect of homogenization practice on the microstructure of AA6063 billets, *J. Mater. Process. Technol.* 148 (2004) 250-258.
- [9] N.C.W. Kuijpers, F.J. Vermolen, K. Vuik and S. van der Zwaag, A Model of the β-AlFeSi to α-Al(FeMn)Si Transformation in Al-Mg-Si Alloys, *Materials Transactions*, 44 (2003) 1448-1456
- [10] K.C. Prince, J.W. Martin, The effects of dispersoids upon the micromechanisms of crack propagation in AlMgSi alloys, *Acta Metall.* 27 (1979) 1401-1408.

- [11] D.H. Lee, J.H. Park, S.W. Nam, Enhancement mechanical properties of Al-Mg-Si alloys by means of manganese dispersoids, *Mater. Sci. Technol* 15 (1999) 450-455.
- [12] Z. Li, Z. Zhang, X.-G. Chen, Effect of magnesium on dispersoid strengthening of Al-Mn-Mg-Si (3xxx) alloys, *Trans. Nonferrous Met. Soc. China* 26 (2016) 2793-2799.
- [13] C. Liu, Microstructure evolution during homogenization and its effect on the high temperature deformation behaviour in AA6082 based alloys, PhD thesis, The university of British Columbia (2017).
- [14] L. Lodgaard, N. Ryum, Precipitation of dispersoids containing Mn and/or Cr in Al-Mg-Si alloys, *Materials Science and Engineering A* 283 (2000) 144-152
- [15] O. Reiso, Extrusion of AlMgSi alloys, *Mater. Forum* 28 (2004) 32-46.
- [16] Y. Birol, The effect of homogenization practice on the microstructure of AA6063 billets, *Journal of Materials Processing Technology* 148 (2004) 250-258
- [17] Y. Birol, Effect of homogenisation cooling rate and press exit temperature on extrudability and T5 hardness of EN AW 6082 alloy, *Materials Science and Technology*, 29 (2013) 1518-1521
- [18] Y. Birol, Effect of cooling rate on precipitation during homogenization cooling in an excess silicon AlMgSi alloy, *Materials Characterization* 73 (2012) 37-42
- [19] X. Qian, N. Parson, X.-G. Chen, Effect of Homogenization Treatment and Microalloying with Mn on the Microstructure and Hot Workability of AA6060 Aluminum Alloys, *Journal of Materials Engineering and Performance*, published online on 25 July 2019, <https://doi.org/10.1007/s11665-019-04232-7>
- [20] M. V. Kral, H.R. McIntyre, M.J. Smillie, Identification of intermetallic phases in a eutectic Al-Si casting alloy using electron backscatter diffraction pattern analysis, *Scripta Materialia* 51 (2004) 215-219.
- [21] H. Tezuka, A. Kamio, L. Arnberg (Ed.), *Aluminum Alloys: Their Physical and Mechanical Properties*, Proceedings of the 3rd International conference (1992) 117-122.
- [22] C. Shi, X.-G. Chen, Effect of vanadium on hot deformation and microstructural evolution of 7150 aluminum alloy, *Materials Science and Engineering A* 613 (2014) 91-102
- [23] H.J. Mc Queen, S. Spigarelli, M. E. Kassner, E. Evagelista, *Hot Deformation and Processing of Aluminum Alloys*, CRC Press, Florida, (2011)
- [24] Q. Hao, M. Lagsvold and B. Olmedal, Comparison of the influence of Si and Fe in 99.999% purity aluminum and in commercial-purity aluminum, *Scripta Materialia*, 67 (2012) 217-220.
- [25] O. D. Sherby, A. Goldberg, O.A. Ruano, Solute-diffusion-controlled dislocation

creep in pure aluminium containing 0.026 at.% Fe, *Philosophical Magazine*, 84 (2004) 2417–2434

[26] O.D. Sherby, O.A. Ruano, Rate-controlling processes in creep of subgrain containing aluminum materials, *Materials Science and Engineering A* 410–411 (2005) 8–11

[27] R. Hu, T. Ogura, H. Tezuka, T. Sato and Q. Liu, Dispersoid Formation and Recrystallization Behavior in an Al-Mg-Si-Mn Alloy, *J. Mater. Sci.* 26 (2010) 237-243

[28] Z. Li, Z. Zhang, X.-G. Chen, Microstructure, elevated-temperature mechanical properties and creep resistance of dispersoid-strengthened Al-Mn-Mg 3xxx alloys with varying Mg and Si contents, *Materials Science & Engineering A* 708 (2017) 383–394